



Research Report

Ion Conductive Organic-inorganic Hybrid Electrolyte with Meso-scale Proton Channels for Fuel Cells

Satoru Fujita, Kazuya Kamazawa, Satoru Yamamoto, Akihiko Koiwai, Shinji Inagaki, Jun Sugiyama and Masaya Kawasumi

Report received on Nov. 13, 2014

■ABSTRACT■ Mesoporous electrolytes construct meso-scale proton-conducting channels by self-assembly of ionic groups such as sulfonic acids in directional pathways. The behavior of proton mobility significantly corresponds to the amount of acid groups and adsorbed water in the mesopores, which play an important role as a proton source and proton carrier under hydrated conditions, respectively. It is noteworthy that the proton diffusivity in the mesopores is enhanced by the higher densification of sulfonic acid groups even at very small amounts of adsorbed water ($H_2O/SO_3H = 2$). Furthermore, under dry conditions, the proton conductivity reaches 0.3 mS cm^{-1} with a surface acid density of up to $3.1 \text{ SO}_3\text{H molecules nm}^{-2}$ at 160°C . This value is higher than that for Nafion by about two orders of magnitude. Such high proton conductivity is considered to be induced by proton hopping within the hydrogen-bonded networks formed by neighboring sulfonic acid groups.

■KEYWORDS■ Organic-inorganic Hybrid, Self-assembly, Meso-scale Ion-conducting Channel, Capillary Condensation of Water, Surface Acid Density, Hydrogen Bond Network, Proton Conductivity

1. Introduction

Fuel cells (FCs) are an important energy conversion technology and have emerged in the last decade as a keystone for future energy supplies.⁽¹⁻³⁾ FCs have attracted much attention as clean energy sources for numerous applications such as electric vehicles, portable electronics and residential power generators, because they exhibit a high power density and efficiency with low emission levels.^(4,5)

However, there are a variety of issues such as cost, durability, heat and water management, that need to be resolved before FC systems can be commercialized widely. To this end, many researchers have focused on electrolytes with high conductivity, electrodes with low Pt loading and membrane-electrode assembly (MEA) designs that are suitable for practical FCs. One of the main challenges in current FC research is to develop an electrolyte that can operate under higher temperature and lower hydration conditions, as an alternative to perfluorosulfonic acid polymers such as Nafion.^(6,7) Generally, proton exchange membranes (PEMs) with high proton conductivity at temperatures between 100 and 200°C are desirable, because operation at higher temperatures can increase catalytic activity, simplify heat and water management, and enhance the tolerance

of the Pt catalysts against CO poisoning.⁽⁸⁾ The key to fast proton transport in electrolytes at high temperature and low water content is thought to lie in constructing the meso-scale morphology of sulfonic acid groups as a proton source, designed so that protons can pass efficiently. However, the continuity of meso-scale proton pathways in perfluorosulfonic acid polymers is almost lost above 100°C and at low water content, resulting in a concomitant decrease in conductivity.

Organic-inorganic hybrid mesoporous materials also form meso-scale ion-conducting channels by self-assembly of ionic groups such as sulfonic acids in directional pathways.⁽⁹⁻¹¹⁾ The most striking characteristic of mesoporous materials with inorganic pore walls is their mechanical and thermal durability. This inorganic wall structure prohibits swelling when hydrated. Moreover, desirable water molecules in the pores are retained by tailoring the sturdy mesostructured channels. Thus, mesoporous materials are expected to exhibit high proton conductivity at higher temperature and lower relative humidity (RH), and allow significant optimization of electrochemical performance.

In this review, we explain the relationship between the proton diffusivity and the water sorption process in uniform meso-scale proton channels of mesoporous

silica materials. Furthermore, we demonstrate the high proton conductivities of mesoporous electrolytes under dry or low RH conditions, and propose a proton conductivity mechanism for the materials on the basis of the results of molecular dynamics (MD) simulations and quasielastic neutron scattering (QENS) measurements.

2. Experimental

2.1 Preparation of Sulfonic Acid-functionalized Mesoporous Electrolytes (Film and Powder)

Sulfonated mesoporous silica films (thickness ≈ 300 nm) were coated on a substrate by the evaporation-induced self-assembly (EISA) approach^(12,13) from precursor mixtures of tetramethoxysilane (TMOS) and 3-mercaptopropyltrimethoxysilane (MPTMS) in the presence of the surfactant alkyltrimethylammonium chloride [$C_nH_{2n+1}N(CH_3)_3Cl$, $n = 12, 14$ and 18] (**Fig. 1**), and treated with H_2O_2 to convert the functional moiety $-SH$ in MPTMS into $-SO_3H$. The films were denoted as MPm-Cn (m is MPTMS content in mol%, and n is alkyl-chain length of surfactant). We also prepared sulfonic acid-functionalized mesoporous silica powders (MP10-C18(p), MP30-C18(p), and MP50-C18(p)) with pore structures and sulfonic acid contents comparable to those of the films (MP10-C18, MP30-C18, and MP50-C18) in order to determine the proton diffusion by QENS measurements, because this was impossible with the thin films.

2.2 Characterizations

2.2.1 Characterizations of Film

Transmission electron microscope (TEM) images were recorded with a JEOL JEM-2000EX instrument at an accelerated voltage of 200 kV. Krypton adsorption-desorption isotherms at $-186^\circ C$ were obtained using a Quantachrome AUTOSORB-1. The ion exchange capacity (IEC) in each electrolyte was confirmed by acid-base titrations. The surface acid density (SO_3H molecules nm^{-2}) in each electrolyte was calculated from IEC and specific surface area obtained by krypton adsorption. The water vapor adsorption-desorption isotherms (water uptakes) of the mesoporous electrolytes was measured using a Quartz Crystal Microbalance (QCM) chip. In-plane proton conductivity of the mesoporous electrolyte on a substrate was measured by electrochemical impedance spectroscopy using a Hioki 3532-50 LCR Hitester instrument. The conductivity was calculated using the following Eq. (1):

$$\sigma = d / (SR), \quad (1)$$

where σ is the conductivity, d is the film thickness, S is the area of cross section, and R is the resistance determined by the intersection of the semicircle in Cole-Cole plots.

MD simulations were carried out to investigate the proton conductive mechanism for the model system

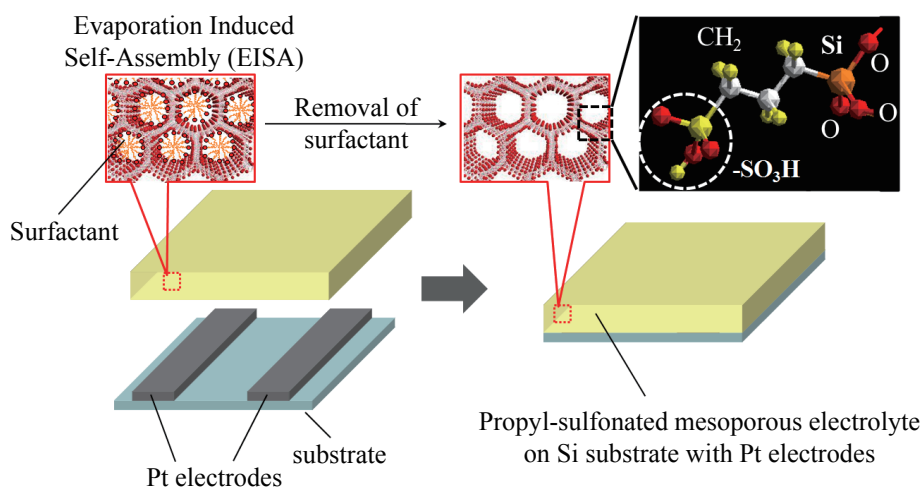


Fig. 1 Procedure of propyl-sulfonated mesoporous silica electrolyte obtained by Evaporation Induced Self-Assembly (EISA) process.

of mesoporous silica electrolyte corresponding to the experimental materials. They were performed using a Forcite module in Materials Studio (Accelrys, Inc.) with a COMPASS forcefield and a Ewald summation method.

2.2.2 Characterizations of Powder

A high-flux backscattering spectrometer (HFBS) at NIST Center for Neutron Research (NCNR)⁽¹⁴⁾ was employed to measure proton diffusion in the powder samples by QENS. A self-diffusion coefficient was calculated by fitting a quasielastic broadening signal at the elastic peak. The line broadening can be modeled in our system with a scattering function $S(Q, \omega)$ given by Eq. (2):

$$S(Q, \omega) = \{\delta(\omega) + e^{-Q^2 \langle u^2 \rangle / 3} L(Q, \omega)\} \otimes R(Q, \omega) + BG, \quad (2)$$

where Q is a momentum transfer, ω is a frequency, and u^2 is an atomic displacement. In the above equation, $R(Q, \omega)$ is an instrumental resolution function, $\delta(\omega)$ is a delta function representing an elastic peak, BG is a background due to atomic vibrations, and $L(Q, \omega)$ is a Lorentzian function that measures a quasielastic broadening with the peak width $\Gamma(Q)$ as given in Eq. (3). We used a vanadium standard for instrumental resolution.

$$L(Q, \omega) = \frac{1}{\pi} \frac{\Gamma(Q)}{[\omega^2 + \Gamma(Q)^2]} \quad (3)$$

3. Results and Discussion

3.1 Characterization of Mesoporous Electrolytes

Figure 2 shows a TEM image of microtome-cut MP40-C18 film embedded in epoxy resin. The cross-sectional image showed a clear hexagonal arrangement of uniform mesopores with a large single crystal-like domain size (at least 500 nm in width), which indicates a highly aligned structure of mesochannels parallel to the substrate surface. The other mesoporous films (MP10-C18, MP30-C18, MP40-C18, -C14, -C12 and MP50-C12) and powders (MP10-C18(p) and MP30-C18(p)) also showed clear TEM images of hexagonal structure and one-dimensional channels (Figs. 3-1(a)-(f) and

3-2(h) and (i)). These results indicate that these mesoporous electrolytes have well-defined and aligned 2D hexagonal mesostructures. On the contrary, the structures of MP50-C18 film and MP50-C18(p) powder showed a disordered phase with a worm-hole structure (Figs. 3-1(g) and 3-2(j)). Table 1 lists IEC for the mesoporous electrolytes. The IEC ranges from 0.78 to 2.30 mmol g⁻¹. These values are almost comparable to the amounts of sulfonate groups in the mesoporous films assuming 100% conversion of SH to SO₃H groups (theoretical IEC = 0.6 – 2.9 mmol g⁻¹). The IEC of MP50-C12 (2.3 mmol g⁻¹) is significantly higher compared to Nafion 112 membrane (0.9 mmol g⁻¹).

3.2 Proton Conductivity under Hydrated Conditions

Figures 4(a) and (b) show the water uptake $\lambda = [\text{H}_2\text{O}] / [-\text{SO}_3\text{H}]$ (25°C) for different RHs of the sulfonated mesoporous silica films. As a comparison, Nafion 112 membrane and Nafion thin film for the adsorption process are also shown. Nafion thin film (thickness: 200 nm) were coated on a substrate using Nafion solution. According to increase in RH, the isotherms of the mesoporous films showed a gentle increase at low RH, a steep increase at medium RH, and almost a plateau at high RH. The gentle increase at low RH is due to the adsorption of water on the pore surface and the clustering around the sulfonic acid groups. The steep increase and the plateau

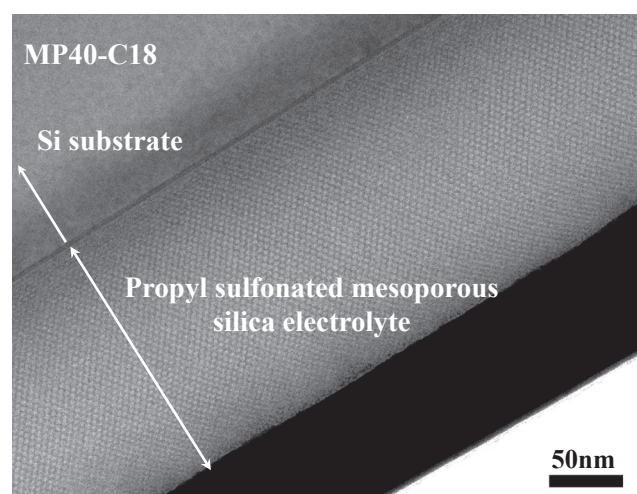


Fig. 2 TEM image of microtome-cut sample for MP40-C18 electrolyte on Si substrate.

correspond to the capillary condensation into the mesopores, and adsorption on the outer surface of the mesoporous films, respectively. At medium RH, the water uptake of the sulfonated mesoporous silica films was significantly higher, by a factor of two, than that of Nafion 112 membrane and Nafion thin film. The onset of capillary condensation shifted to lower RH upon decreasing pore size or increasing IEC of the sulfonated mesoporous film. The RH shift could be explained reasonably by the following Kelvin Eq. (4):

$$\ln(P/P_0) = -2\gamma V_m \cos\theta / (rRT), \quad (4)$$

where P/P_0 is a relative vapor pressure at capillary

condensation, γ and V_m are a surface tension and a molecular molar volume of water, respectively, r is a pore radius, R and T are a gas constant and an absolute temperature, respectively, and θ is a contact angle between the pore surface and water molecule. According to the Kelvin equation, P/P_0 becomes small with decreases in r and θ . The increase in IEC in the mesopore surface decreases θ due to the hydrophilic property of the sulfonic acid group and r due to the bulkiness. Therefore the increase in IEC causes the capillary condensation at lower RH. Figure 4(c) shows proton conductivity of the sulfonated mesoporous films as a function of RH. The proton conductivities were very high ($6.0 \times 10^{-3} - 3.4 \times 10^{-2} \text{ S cm}^{-1}$) at

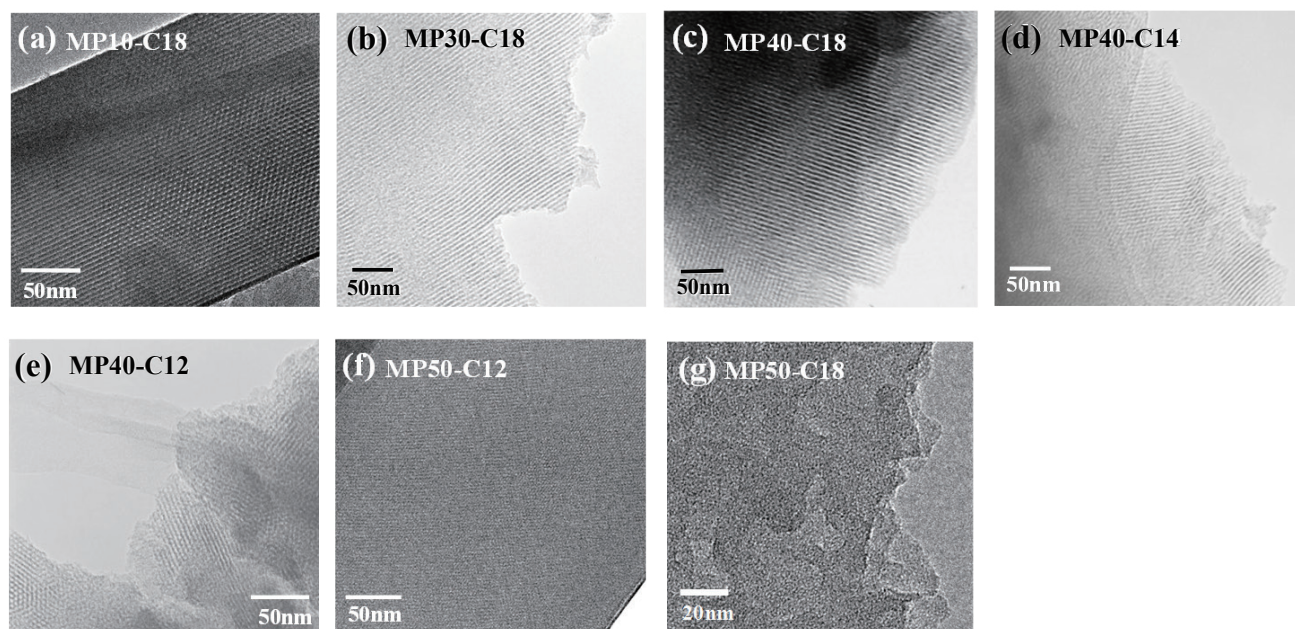


Fig. 3-1 TEM images of propyl-sulfonated mesoporous silica films; (a) MP10-C18, (b) MP30-C18, (c) MP40-C18, (d) MP40-C14, (e) MP40-C12, (f) MP50-C12 and (g) MP50-C18.

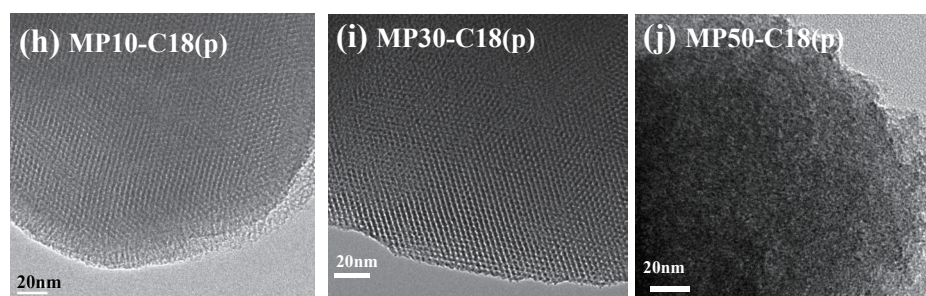


Fig. 3-2 TEM images of propyl-sulfonated mesoporous silica powders; (h) MP10-C18 (p), (i) MP30-C18 (p) and (j) MP50-C18 (p).

high RH where the mesopores were filled with water completely. The proton conductivity jumped and dropped 2-3 orders of magnitude at medium RH in accordance with the steep increase and decrease in adsorption of water, respectively. RH at the steep change in proton conductivity shifted lower with the decrease in pore size and increase in IEC, which corresponded well with the water vapor adsorption-desorption isotherms. Thus, the RH position at the steep change can be controlled by the pore size and the IEC of mesoporous silica according to the Kelvin equation. **Figure 5** shows the relationship between proton diffusion coefficient (D_σ) and water filling ratio (F_p) in the mesopores. The D_σ were calculated using the Nernst-Einstein Eq. (5):

$$D_\sigma = kT\sigma/N_H e^2, \tag{5}$$

$$N_H = (\rho IEC/1000)N_A, \tag{6}$$

where k is a Boltzmann's constant, T is an absolute temperature, σ is a proton conductivity, N_H (Eq. (6)) is a concentration of the protonic volume calculated from the IEC value, e is an electric charge, N_A is Avogadro's constant, and ρ is a density of the film calculated from the weight and the thickness of the film on the substrate. The F_p were calculated by the following Eq. (7):

$$F_p = V_w/V_p, \tag{7}$$

where V_w and V_p are a volume of adsorbed water and

Table 1 Physicochemical properties of sulfonic acid mesoporous silica.

Sample	Meso struct.	S_{BET} , $m^2 \cdot g^{-1}$	Pore Volume, $cc \cdot g^{-1}$	Pore Diameter, nm	IEC*, $mmol \cdot g^{-1}$	Surface acid density, $molecules \cdot nm^{-2}$
MP10-C18	2d-hex	620	0.51	3.9	0.78 (0.6)	0.75
MP10-C18(p)	2d-hex	1087	1.27	3.1	0.47(0.6)	0.22
MP30-C18	2d-hex	756	0.40	3.4	1.52 (1.7)	1.18
MP30-C18(p)	2d-hex	941	0.78	2.1	1.52 (1.7)	0.96
MP40-C18	2d-hex	810	0.36	3.2	1.80 (2.3)	1.34
MP40-C14	2d-hex	910	0.27	3.0	1.82 (2.3)	1.20
MP40-C12	2d-hex	830	0.26	2.7	1.80 (2.3)	1.31
MP50-C12	2d-hex	980	0.30	2.2	2.30 (2.9)	1.41
MP50-C18	Wormhole	390	0.15	1.7	2.25 (2.9)	3.10
MP50-C18(P)	Wormhole	531	0.61	2.0	2.21 (2.9)	2.51

*() theoretical IEC

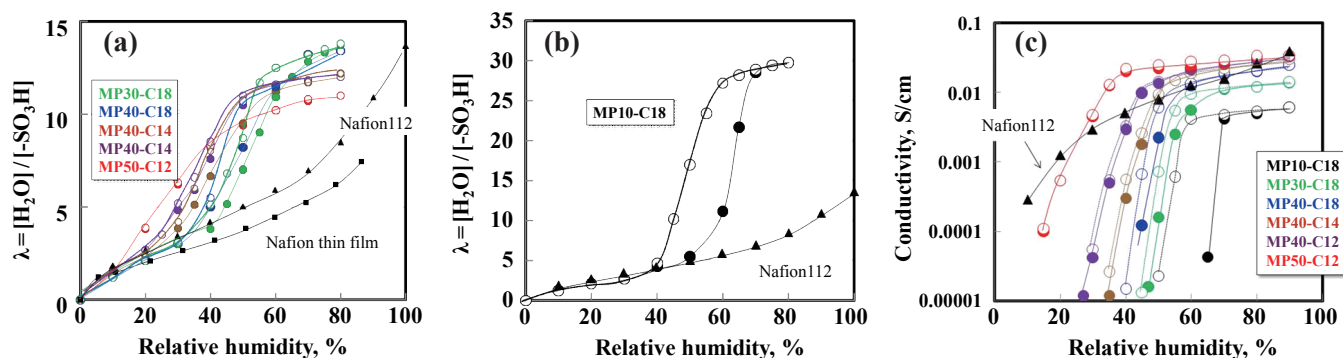


Fig. 4 Water uptakes (a), (b) and proton conductivities (c) of propyl-sulfonated mesoporous silica films at 25°C various different RH values. Solid and open circles show water adsorption and desorption processes, respectively. Nafion112 and Nafion thin film only water uptakes for adsorption process are shown ((a), (b)).

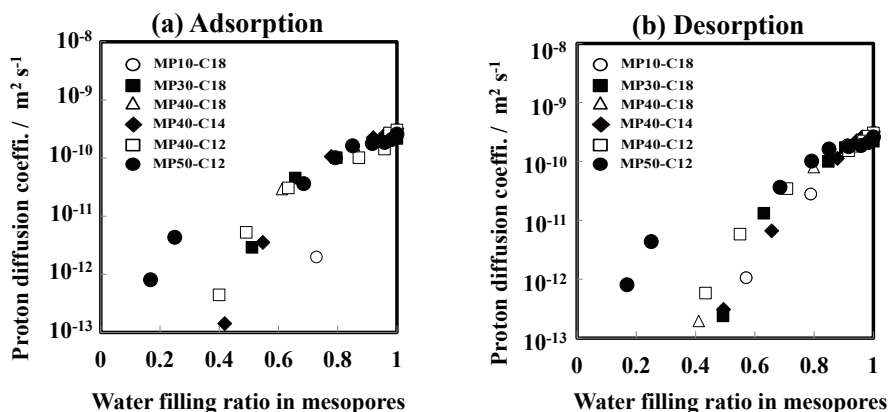


Fig. 5 The relationship between proton diffusion coefficient and water filling ratio in mesopores for propyl-sulfonated mesoporous silica films.

a pore volume, respectively. D_{σ} steeply increased at around $F_p = 0.4$ and reached the maxima at $F_p = 1$ for the mesoporous films except for MP50-C12 and MP10-C18. This indicates that more than 40% filling of mesopores with water is necessary for exhibiting high diffusion of protons for mesoporous films with moderate IEC and pore sizes. Surprisingly, MP50-C12 showed a steep increase in D_{σ} at around $F_p = 0.2$. Only 20% filling of mesopores is enough for exhibiting high proton diffusion. This is mainly attributed to the high IEC (2.3 mmol g⁻¹, Table 1). The high IEC can make proton channels effective with a smaller amount of water (**Fig. 6(a)**). MP10-C18 with low IEC (0.78 mmol g⁻¹, Table 1) showed an increase in D_{σ} at around $F_p = 0.7$ because a large amount of water is necessary to make the proton channels effective (**Fig. 6(b)**).

Figure 7 shows proton conductivities of MP50-C12 at various RHs (90, 50, and 20%) above 25°C, and Arrhenius plots of the conductivities and activation energies (E_a). The proton conductivities increased with increasing temperature, and indicated high proton

conductivities of 0.16, 0.11, and 0.0041 S cm⁻¹ for RH 90, 50, and 20%, respectively at 100°C. The E_a was obtained by linear regression of an Arrhenius Eq. (8):

$$\sigma = \sigma_0 \exp(-E_a/k_b T), \quad (8)$$

where σ_0 is a pre-exponential parameter and k_b is Boltzmann's constant. The values of E_a at RH 20, 50, and 90% were estimated to be 0.26, 0.20, and 0.19 eV, respectively. These values indicate a Grotthuss mechanism for the proton conduction. Activation energy values typically attributed to Grotthuss transfer via water molecules are in the range of 0.14 – 0.40 eV.⁽¹⁴⁾ The magnitude of E_a decreased with increasing RH, because water molecules as mobile species were introduced.

3.3 Proton Conductivity under Dry Condition

Figure 8(a) shows proton conductivities of MP30-C18 and MP50-C18 films with different IEC above 100°C, and under dry (RH 0%) or low RH condition. In **Fig. 8**, the data for Nafion 112 (IEC = 0.9 mmol g⁻¹) and sulfonated polystyrene (SPS) (IEC = 5.37 mmol g⁻¹) measured under dry condition are shown for comparison. Under dry condition, proton conductivities of both MP30-C18 and MP50-C18 increased with increase in temperature. Comparing the data obtained under dry condition, it is very clear that proton conductivity of MP50-C18 with high IEC (2.25 mmol g⁻¹) was higher than that of MP30-C18 (1.52 mmol g⁻¹). Consequently, proton

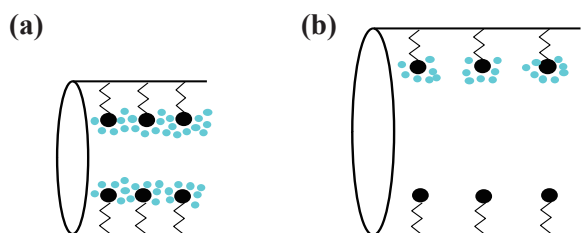


Fig. 6 Water sorption at (a) high and (b) low acid density at low RH and proton channel formation.

conductivity is found to be enhanced by the high IEC by about two orders of magnitude compared with that of MP30-C18. Furthermore, the proton conductivity of MP50-C18 was higher than that of Nafion by one order of magnitude. It is worth noting that MP50-C18 has conductivity comparable to that of SPS, although the IEC in MP50-C18 is lower than that of SPS (5.37 mmol g⁻¹). This indicates that the continuity of proton pathways for mesoporous electrolyte is sustained by inorganic pore walls even at high temperature and low water content allowing for a high proton conductivity, in the case of Nafion and SPS, the proton pathways is almost lost.

The values of E_a for MP30-C18 and MP50-C18

are estimated to be 0.47 and 0.45 eV, respectively, under dry condition (Fig. 8(b)). This demonstrates that the increase in the surface acid density in pores reduce E_a for anhydrous proton transfer. This shows that the increase in IEC reduces E_a for anhydrous proton transfer. This also agrees with the results of the energy barrier of proton transfer calculated by the MD simulation.⁽¹⁵⁾ In order to consider the actual proton transfer in pores, “surface acid density” is more appropriate than IEC, because the former includes pore information and the latter does not. Therefore the surface acid density is used instead of IEC hereafter. **Figure 9** shows detailed atomistic surface models of the silica walls with various surface acid densities.

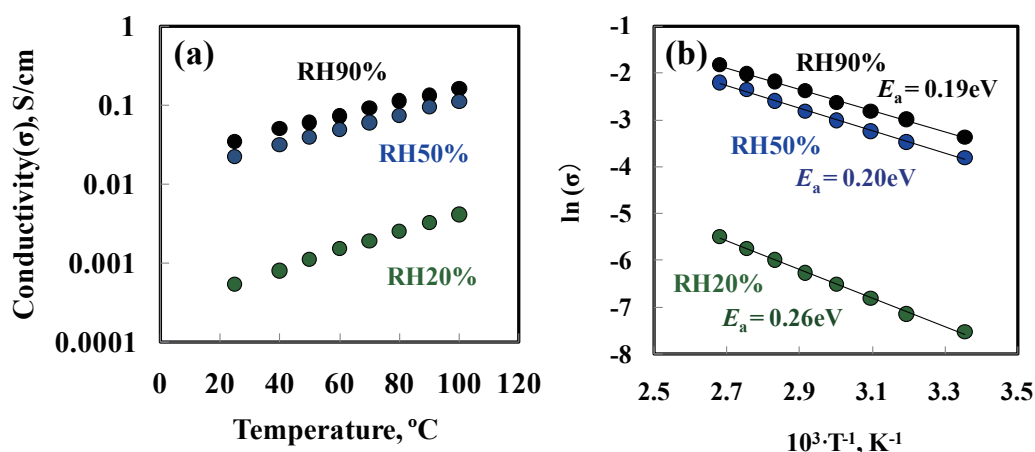


Fig. 7 (a) Proton conductivities of MP50-C12 at various RH (90, 50, and 20%) above 25°C and (b) Arrhenius plots of the conductivities and activation energies (E_a) of MP50-C12.

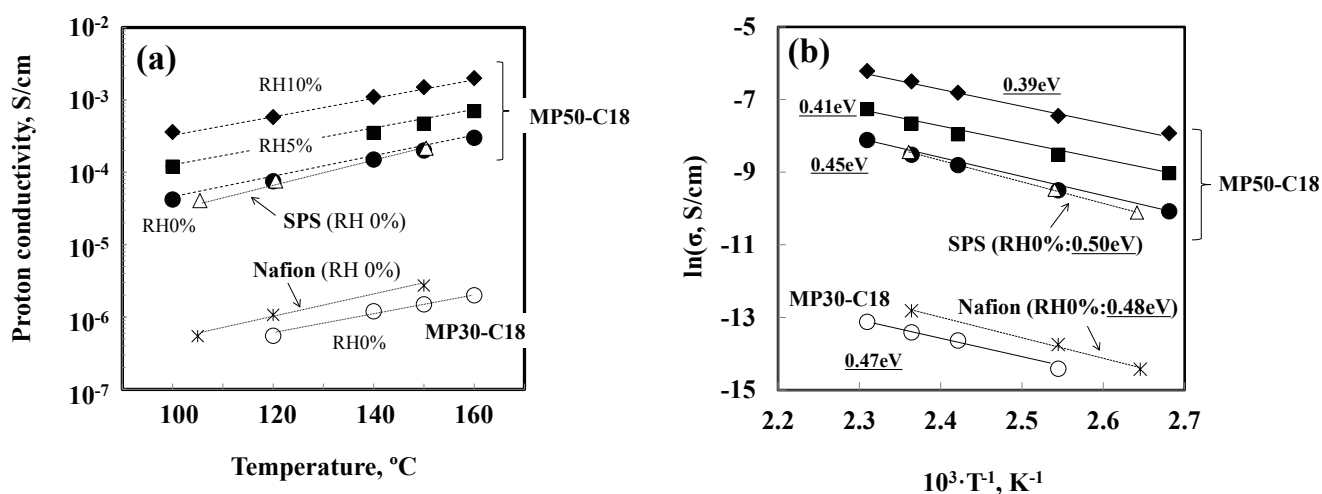


Fig. 8 (a) Proton conductivities of various electrolytes under different RH conditions above 100°C, (b) Arrhenius plots of the conductivities and activation energies (E_a) of various electrolytes. E_a was estimated from the slope.

Below 1.5 SO_3H molecules nm^{-2} , the sulfonic acid groups formed hydrogen bonds only to the OH groups on the silica surface. Above 2.0 SO_3H molecules nm^{-2} , the hydrogen bonds constructed a continuous network even at 25°C. This means that the proton conduction pathways are connected throughout the entire surface by a hydrogen bond network, resulting in the suppression of E_a for the proton jumping from one sulfonic acid site to the nearest neighboring sulfonic acid site even under dry condition. On the other

hand, the values of E_a for Nafion and SPS under dry condition are 0.48 and 0.50 eV, respectively. These values are higher than the values for MP30-C18 and MP50-C18. These data show the importance of proton channel continuity in the electrolytes. The mesoporous electrolyte has a rigid silica mesopore backbone that supports the presence of sulfonic acid groups at high density within the pores. This construction allows proton channel continuity in the pores even under dry condition, and permits proton transfer with

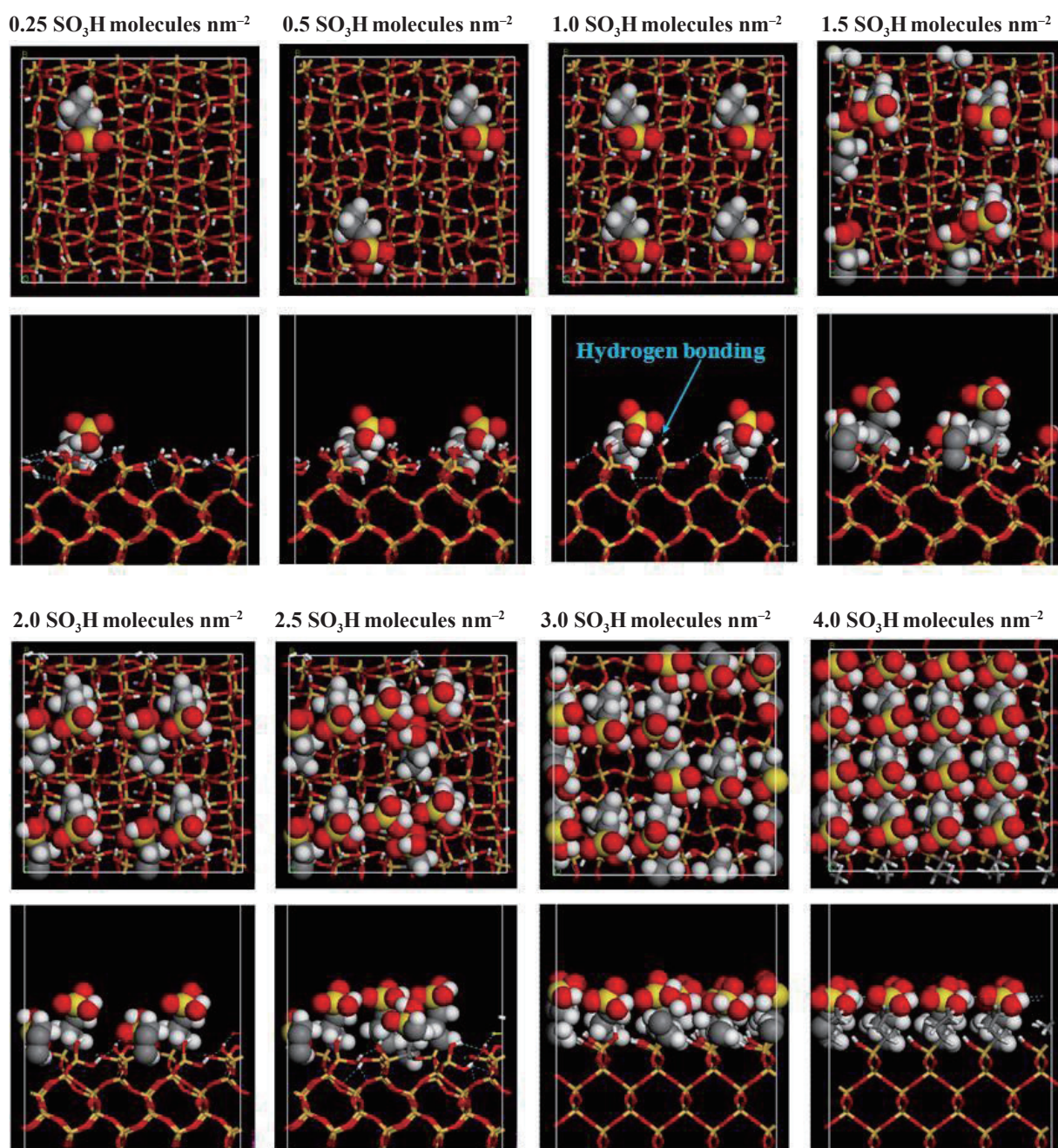


Fig. 9 Atomic surface models on the silica walls with various acid density (0.25-4.0 SO_3H molecules nm^{-2}).

lower E_a compared with Nafion and SPS electrolytes. Based on MD simulations, proton conduction takes place predominantly via the hydrogen bonds of the sulfonic acid groups. Furthermore, this high proton conductivity of mesoporous materials is strongly related to a high density of SO_3H groups. Under a small amount of water, i.e., 5 and 10% RH, proton conductivity of MP50-C18 was drastically enhanced compared with the dry condition (Fig. 8). In fact, proton conductivity was 2 mS/cm at 160°C in the case of 10% RH. The magnitude of E_a also decreased with increasing humidity (0.41 and 0.39 eV for RH 5 and 10%), due to added water molecules as proton carriers. The mesoporous electrolytes loaded with sulfonic acid groups at high surface acid density are, therefore, found to promote efficient proton transport even under low RH conditions.

3.4 Quasielastic Neutron Scattering

Figure 10(a) shows the variation of the QENS spectra with various surface acid densities, namely, the spectra for MP10-C18(p), MP30-C18(p), MP50-C18(p) and mesoporous silica (MS) without SO_3H groups at 27°C. It is clear that the QENS spectrum becomes broad with increasing surfaced acid density. From this, we can conclude that broadened spectra are due to hydrogen motions in sulfonic acid. The spectrum of MP50-C18(p) with high surface acid density of 2.5 SO_3H molecules nm^{-2} at 97°C is shown in Fig. 10(b) as compared with that at 27°C. The QENS spectrum also becomes broad with increasing temperature. The quasielastic scattering is fitted well by delta and Lorentz functions (Eq. (2)) convoluted with instrumental resolution. The Q dependence of the obtained full width at half maximum (FWHM) ($\Gamma_{\text{FWHM}}(Q)$) of the Lorentzian (Eq. (3)) for MP50-C18(p) at 97°C is shown in Fig. 10(c). The curve is fitted well by a jump diffusion model. This indicates that the proton of a sulfonic acid group can self-diffuse even in the absence of water, as in the case for superprotonic conductors.⁽¹⁶⁾ A numerical values of proton self-diffusion coefficient (D), an average diffusion length (ℓ) and a residence times (τ) obtained from the fitting curve of Fig. 10(c) are $9.11 \times 10^{-6} \text{ cm}^2 \text{ sec}^{-1}$, 0.43 nm and $3.5 \times 10^{-9} \text{ sec}$, respectively. The diffusion length of proton self-diffusion obtained by QENS measurements is 0.43 nm, which is consistent with distance to the nearest neighboring sulfonic acid site

($\approx 0.4 \text{ nm}$ for 2.5 – 3.0 SO_3H molecules nm^{-2}) obtained by the present MD simulations. Based on the results of macroscopic proton conductivities for MP50-C18 (3.1 SO_3H molecules nm^{-2}), the following model is proposed. Under anhydrous condition, the continuity of the hydrogen bond network is maintained by high densification of sulfonic acid groups. As for proton transport, proton conduction seems to be related

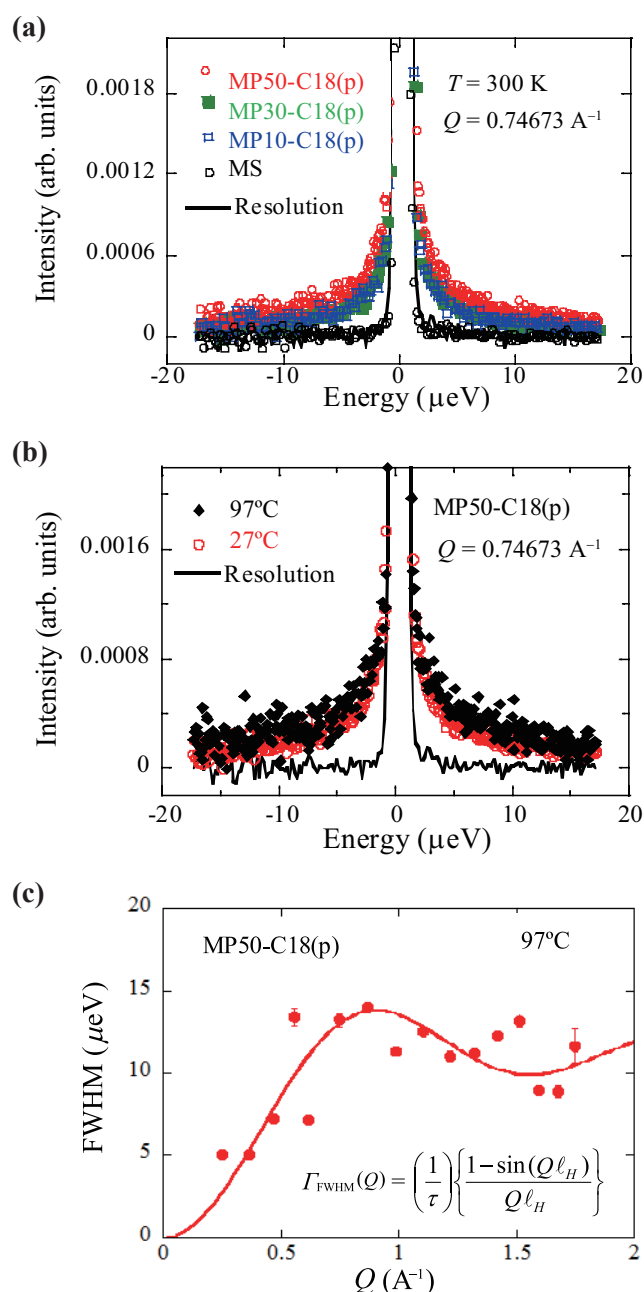


Fig. 10 (a) QENS spectra at 27°C of MP10-C18(p), MP30-C18(p) and MP50-C18(p). (b) Temperature dependences of QENS spectra of MP50-C18(p). (c) FWHM v.s. Q for 97°C of MP50-C18(p) using a jump diffusion model.

to proton self-diffusion of the sulfonic acid group within the hydrogen bond network. It can therefore be presumed that the distances of proton transport are elongated by increasing the number of neighbors in the vicinity of the sulfonic acid site. Thus, the high concentration of hydrogen bonds, which are formed by highly dense sulfonic acid groups, is necessary to increase anhydrous proton conductivity efficiently.

4. Conclusion

The mesoporous silica electrolytes are of great advantage in that a large amount of sulfonic acid groups can be incorporated in the mesopores with no swelling and dissolution properties while preserving the uniform pore structure. Under hydrated conditions, the proton conductivity increased steeply at medium RH according to the capillary condensation of water in the uniform mesopores. The proton conductivities are enhanced by the high densification of sulfonic acid groups even at very small amounts of adsorbed water. Furthermore, under dry condition, the continuity of a hydrogen bond network is built by the high densification of sulfonic acid groups, and such network is thought to induce proton hopping conduction between the neighboring sulfonic acid groups. Such network presumably enhanced proton transport through the pore channels, resulting in high proton conductivity at high temperatures. The information gleaned from this study will be useful for further understanding of proton diffusivity in meso-scale channels.

References

- (1) Steel, B. C. H. and Heintzel, A., *Nature*, Vol. 414 (2001), pp. 345-352.
- (2) Kreuer, K. D., *Chem. Mater.*, Vol. 8 (1996), pp. 610-641.
- (3) Diat, O. and Gebel, G., *Nature Mater.*, Vol. 7 (2008), pp. 13-14.
- (4) Mehta, V. and Cooper, J. S., *J. Power Sources*, Vol. 114 (2003), pp. 32-53.
- (5) Martin, W. and Ralph, J. B., *Chem. Rev.*, Vol. 104 (2004), pp. 4245-4269.
- (6) Kreuer, K. D., Paddison, S. J., Spohr, E. and Schuster, M., *Chem. Rev.*, Vol. 104 (2004), pp. 4637-4678.
- (7) Hickner, M. A., Ghassemi, H., Kim, Y. S., Einsla, B. R. and McGrath, J. E., *Chem. Rev.*, Vol. 104 (2004), pp. 4587-4612.
- (8) Li, Q., He, R., Jensen, J. O. and Bjerrum, N. J., *Chem. Mater.*, Vol. 15 (2003), pp. 4896-4915.
- (9) Marschall, R., Rathouský, J. and Wark, M., *Chem. Mater.* Vol. 19 (2007), pp. 6401-6407.
- (10) McKeen, J. C., Yan, Y. S. and Davis, M. E., *Chem. Mater.*, Vol. 20 (2008), pp. 5122-5124.
- (11) Marschall, R., Tölle, P., Cavalcanti, W. L., Wilhelm, M., Köhler, C., Frauenheim, T. and Wark, M., *J. Phys. Chem. C*, Vol. 113 (2009), pp. 19218-19227.
- (12) Ogawa, G., *Chem. Commun.* (1996), pp. 1149-1150.
- (13) Brinker, C. J., Lu, Y., Sellinger, A. and Fan, H., *Adv. Mater.*, Vol. 11, No. 7 (1999), pp. 579-585.
- (14) Colomban P. and Novak, A., *Proton Conductors*, (1992), pp. 38-55, Cambridge University.
- (15) Marschall, R., Tölle, P., Cavalcanti, W. L., Wilhelm, M., Köhler, C., Frauenheim, T. and Wark, M., *J. Phys. Chem. C*, Vol. 113 (2009), pp. 19218-19227.
- (16) Kamazawa, K., Harada, M., Ikedo, Y., Sugiyama, J., Tyagi, M. and Matsuo, Y., *J. Phys. Soc. Jpn.*, Vol. 79, Suppl. A (2010), pp. 7-11.

Figs. 1, 2 and 4-7

Reprinted and modified from *Chem. Mater.*, Vol. 25 (2013), pp. 1584-1591, Fujita, S., Koiwai, A., Kawasumi, M. and Inagaki, S., Enhancement of Proton Transport by High Densification of Sulfonic Acid Groups in Highly Ordered Mesoporous Silica, © 2013 ACS, with permission from American Chemical Society.

Figs. 8-10

Reprinted and modified from *J. Phys. Chem. C*, Vol. 117 (2013), pp. 8727-8736, Fujita, S., Kamazawa, K., Yamamoto, S., Tygi, M., Araki, T., Sugiyama, J., Hasegawa, N. and Kawasumi, M., Proton Conductivity under Dry Conditions for Mesoporous Silica with Highly Dense Sulfonic Acid Groups, © 2013 ACS, with permission from American Chemical Society.

Sections 3.1 and 3.2

Reprinted from *Chem. Mater.*, Vol. 25 (2013), pp. 1584-1591, Fujita, S., Koiwai, A., Kawasumi, M. and Inagaki, S., Enhancement of Proton Transport by High Densification of Sulfonic Acid Groups in Highly Ordered Mesoporous Silica, © 2013 ACS, with permission from American Chemical Society.

Sections 3.3 and 3.4

Reprinted from *J. Phys. Chem. C*, Vol. 117 (2013), pp. 8727-8736, Fujita, S., Kamazawa, K., Yamamoto, S., Tygi, M., Araki, T., Sugiyama, J., Hasegawa, N. and Kawasumi, M., Proton Conductivity under Dry Conditions for Mesoporous Silica with Highly Dense Sulfonic Acid Groups, © 2013 ACS, with permission from American Chemical Society.

Satoru Fujita

Research Fields:

- Solid State Ionics
- Inorganic Chemistry

Academic Degree: Dr.Eng.

Academic Society:

- The Solid State Ionics Society of Japan

**Shinji Inagaki**

Research Field:

- Synthesis and Applications of Mesoporous Materials

Academic Degree: Ph.D.

Academic Societies:

- The Chemical Society of Japan
- Catalysis Society of Japan
- Japan Association of Zeolite
- The Japan Society on Adsorption
- The Society of Polymer Science, Japan
- International Mesoporous Materials Association
- International Zeolite Association

Awards:

- The Award of Chemistry on Catalyst Preparation, 1994
- The Promotion Award of the Japan Society on Adsorption, 2001
- The Chemical Society of Japan Award for Creative Work, 2004
- The Minister Award of Education, Culture, Sport, Science and Technology, 2005
- The Japan Society on Adsorption Award, 2008

**Kazuya Kamazawa**

Research Field:

- Neutron Scattering Experiments

Academic Degree: Dr.Sci.

Academic Societies:

- The Physical Society of Japan
- The Japanese Society for Neutron Science

Present Affiliation: Comprehensive Research Organization for Science and Society

**Satoru Yamamoto**

Research Fields:

- Computational Chemistry for Materials
- Rheology of Polymer and Suspension

Academic Degree: Dr.Eng.

Academic Societies:

- The Society of Polymer Science, Japan
- The Society of Rheology Japan

Awards:

- R&D 100 Award (Fillers Flow), 1999
- Research Award of the Soc. of Rheology Japan, 2001

Present Affiliation: Dassault Systemes Biovia K. K.

**Jun Sugiyama**

Research Field:

- Materials Analysis using Muons and Neutrons

Academic Degree: Dr.Eng.

Academic Societies:

- Physical Society of Japan
- American Physical Society
- Society of Muon and Meson Science of Japan
- International Society for μ SR Spectroscopy
- The Japanese Society for Neutron Science

Awards:

- Best Poster Award of International Conference on Neutron Scattering, 2013
- World Young Fellow Meeting Presentation Award of The Ceramic Society of Japan, 2004

**Akihiko Koiwai**

Research Fields:

- Materials Science
- Fuel Cell

Academic Societies:

- The Chemical Society of Japan
- The Society of Polymer Science, Japan

**Masaya Kawasumi**

Research Fields:

- Fuel Cell
- Macromolecular Science
- Polymer Synthesis

Academic Degree: Ph.D.

Academic Societies:

- The Chemical Society of Japan
- The Society of Polymer Science, Japan
- The Electrochemical Society of Japan

Awards:

- The Award of the Society of Polymer Science, Japan, 2009
- The Society of Silicon Chemistry Japan Award, 2007

